Computational Mathematical Modelling of Sound Propagation in Ducted Silencers

Sara Brandberg

May 1999

MASTER'S THESIS

Examiner
Kenneth Eriksson

Department of Mathematics
CHALMERS UNIVERSITY OF TECHNOLOGY
GÖTEBORG UNIVERSITY
Göteborg Sweden 1999

Abstract

Sound propagation through a silencer for noise reduction in a ventilation duct is studied using computational mathematical modelling based on Helmholtz equation and the finite element method.

Computations of the sound reduction/insertion loss for the ducted silencer is compared to measurements from experiments with good coincidence. Frequencies above the cut-on frequency are reduced more in the measured case than in the computed one because the theoretical solution does not include non-axial wave modes. The curves oscillate at the lower frequencies depending on standing waves caused by reflections. In the measured case this effect is not that obvious because the oscillations are smoothened out.

The silencer length, the duct radius and the flow resistivity together with the thickness of the material in the silencer have the greatest impact on the insertion loss.

Sammanfattning

Vågutbredning i ljuddämpare för bullerreduktion i ventilationsrör studeras med en matematisk modell baserad på Helmholtz ekvation och finita elementmetoden.

Insättningsdämpning för det beräknade och mätta fallet jämförs med bra resultat. Frekvenser över den så kallade cut-on frekvensen reduceras mycket bättre i det mätta fallet jämfört med det beräknade på grund av att tvärmoder inte produceras i modellen av källan. Kurvorna oscillerar i de låga frekvensbanden vilket beror på att stående vågor uppkommer på grund av reflektion av vågor. Dessa effekter är inte lika tydliga i det mätta fallet eftersom sådana hopp jämnas ut av ojämnheter i systemet.

Ljuddämparens längd, kanalens radie och ljuddämparmaterialets flödesresistans tillsammans med dess tjocklek utgör de parametrar som påverkar insättningsdämpningen mest.

Preface

This report is my graduate thesis for the degree of Master of Science completing Problem Solving in Science at Göteborg University. It is a project initialized at the Acoustic section at Swedish National Testing and Research Institute by Hans Jonasson.

The work has been supervised by Kenneth Eriksson at Chalmers University of Technology and Göteborg University, who has inspired me and been of great support during these months. I am also grateful for all the time, good advise and expert help that I received from Mikael Ögren and Hans Jonasson at Swedish National Testing and Research Institute.

Sara Brandberg

Contents

1 Nomenclature

Roman letters

A	matrix
b	dissipative constant
c	sound velocity, ms^{-1}
d	duct diameter, m
`e`	a matrix describing the triangle edges of the triangulation of the domain coinciding with the boundary of the domain
f	frequency, Hz; force, N; source term
F	force, N
`g`	a matrix for the domain of computation
k	wave number, m^{-1}
k_s	spring constant
L_p	sound pressure level, dB
m	mass, kg
$\mathbf{n}$	normalised vector
p	sound pressure, Pa
$\hat{p}$	time dependent sound pressure, Pa
`p`	a 2×N matrix of all the z and r values for the nodes of the triangulation of the domain
p_I	known sound pressure at the inlet of the duct
p_i	P's values on the node points
P	p's projection on a triangulation of the domain
$\mathbf{P}$	vector with the elements p_i
r	variable in the radial direction of the duct, m
r_{max}	radius of the duct, m
S	area, m^2
`t`	a matrix with one column for each triangle of the triangulation of the domain in the mesh specifying its three node numbers
t_{abs}	the thickness of the absorbing material, m
t_{metal}	the thickness of the perforated metal, m
u	particle velocity, ms^{-1}
U	velocity, ms^{-1}
z	variable in the length direction of the duct, m
z_1	the inlet coordinate of the silencer on the z axis, m
z_2	the outlet coordinate of the silencer on the z axis, m
z_{max}	the length of the duct, m
Z	acoustic impedance, Nsm^{-5}

Greek letters

φ	test function
λ	wavelength, m
ω	angular frequency s^{-1}
Ω	cross section of the duct
ρ	density, kgm^{-3}
σ	flow resistivity, $kgs^{-1}m^{-3}$
χ	test function

2 Explanations of some important words

Acoustic impedance is the complex ratio of the effective sound pressure at a point of an acoustic medium and the effective particle velocity at that point, $\frac{p}{u}$.[1]

Cut-on frequency is the frequency above which non-axial wave modes can propagate through a duct. This is when the wave length is equal to 0,58 times the duct diameter ($\lambda = 0,58d$).

Insertion loss is the difference between the sound pressure levels before and after the silencer is installed.

Sound pressure level is calculated as $L_p = 20 \log \frac{|p|}{|p_0|}$, where $p_0 = 20\mu Pa$ is a reference pressure corresponding to $L_p = 0$.

[1] Beranek, 1986

3 Introduction

Ventilation ducts, unfortunately, guide not only the ventilation air but also sound waves, for example from the ventilation fan, which can be experienced as noise to the human ear. Ventilation ducts can also unintentionally guide sound waves from one room to another in a building. Because of this, ventilation ducts are often equipped with silencers to reduce the sound propagation through the system, while keeping an open channel for the ventilation air flow.

Silencer prototypes are tested at SP, Swedish National Testing and Research Institute for performance data. Such a test requires resources in terms of space, machinery, personal and time. The purpose of this work is to study the possibility to replace or complement the experimental testing with evaluations of the performance of silencer through computational mathematical modelling. In this report sound propagation in a duct is modelled by the finite element method and the insertion loss of ducted silencers is computed.

The advantage of using a computational tool compared to an experimental setup is that we may easily visualize various phenomena to better understand how silencers interact with the wave propagation. We may also perform a large number of computational experiments fast and at low cost, because in the computer we can rebuild the setup just by varying parameters.

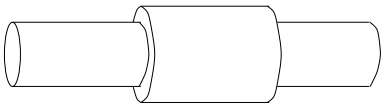

Figure 1: Duct with silencer.

4 Construction of a silencer

An exterior view of a duct with a silencer is sketched in Figure 1. The type of silencer considered in this report is built up by some absorbing material, like mineral wool and sheet metal (some of it perforated). The perforated sheet metal forms a cylinder with the same radius as the duct and a layer of the absorbing material is put between the perforated sheet metal and a bigger cylinder of sheet metal, see Figure 2.

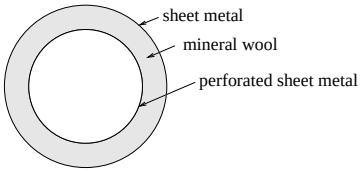

Figure 2: A cross section of a silencer.

5 Mathematical modelling

5.1 Helmholtz equation

The propagation of sound is governed by the wave equation

$$\Delta \hat{p} - \frac{1}{c^2}\frac{\partial^2 \hat{p}}{\partial t^2} = 0 \tag{1}$$

where $\hat{p} = \hat{p}(x, y, z, t)$ is the sound pressure fluctuation, depending on the space coordinates x, y, z and the time t, Δ is the Laplace operator of second space derivatives, and c is the sound velocity in the medium of transportation (here air).

Since the wave equation is linear we may study the response of the system for each frequency separately. We shall therefore consider given pressure fluctuation of the form $\cos(\omega t)$ at the inlet (to the left) of the section of the ventilation duct in Figure 1 ($\omega = 2\pi f$ and f is the frequency). With given data of this form it is natural to seek a solution of the form $\hat{p} = Re(pe^{-i\omega t})$, where $p = p(x, y, z)$ is the time independent sound pressure. When this is inserted into the wave equation (1) we obtain the Helmholtz equation

$$\Delta p + k^2 p = 0 \tag{2}$$

where k, called the wave number, equals $\frac{\omega}{c}$. We are thus left with a time independent equation where the frequency enters through the coefficient k in the equation.

5.2 Boundary conditions

The boundary conditions are given by a known pressure p_I at the inlet of the duct, and by the Robin condition

$$p + \frac{1}{i\omega\rho} Z \mathbf{n} \cdot \nabla p = 0 \tag{3}$$

on the sides and at the outlet of the duct. Here ρ is the density of the medium (here air), $\mathbf{n}$ is the unit normal from the boundary pointing out from the duct, Z is the so called acoustic impedance, and ∇ is the gradient operator of derivatives in the x, y and z directions.

When a force $f = Fe^{-i\omega t}$ is applied to a mechanical system composed of the three components in Figure 3, the system will be accelerated, receive a velocity and be displaced. This responds with a force

$$f = m\ddot{x} + b\dot{x} + k_s x = (-m\omega^2 + bi\omega + k_s)Xe^{-i\omega t} =$$

$$= [b + i(\frac{k_s}{\omega} - m\omega)](-i\omega X)e^{-i\omega t} = ZUe^{-i\omega t} = Zu,$$

where $x = Xe^{-i\omega t}$ is the displacement, $\dot{x} = -i\omega t Xe^{-i\omega t}$ the velocity, $m\ddot{x}$ the inertia force, $b\dot{x}$ dissipative friction force in the piston, and $k_s x$ elastic deformation force in the spring. The ratio $\frac{F}{U} = Z_m$ is called the (mechanical) *impedance*. We note, in particular, that $|U|$ is maximal when $|Z|$ is minimal, that is when $\frac{k_s}{\omega} - m\omega$ is zero, referred to as resonance.

Similarly, when a pressure force $p = Pe^{-i\omega t}$ is exerted to a material, the material will respond with a force $Z_a Ue^{-\omega t}$ where the ratio $\frac{P}{U} = Z_a$ is the *acoustic impedance* of the material. Like the mechanical impedance, the acoustic impedance has a real part corresponding to dissipative force, and an imaginary part corresponding to reactive forces.

This analogy between mechanical and acoustic impedance is only valid when the acoustic components (e.g. the duct diameter) are smaller than the wave length, but it is useful as basis for understanding the acoustic impedance.

At the outlet of a duct reflections may be formed which we wish to suppress so that the effect of the silencer may be studied more easily. This can be accomplished through particular so called absorbing boundary conditions at the outlet yielding no reflection. If we put the acoustic impedance Z to ρc, which is the same impedance as air[2], in the Robin condition (3) that will result in complete transmission of incoming waves modelling that the duct

[2]Kinsler et al, 1982

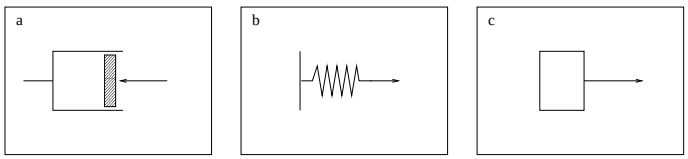

Figure 3: A mechanical system composed by (a) a damped piston, (b) a spring and (c) a mass can be used as an analogy to acoustic impedance.

continues.

The Robin condition (3) is also used for the segment on the boundary where the silencer is supposed to be. The acoustic impedance of the silencer is dependent on the frequency and on the construction and the material of the silencer.

On the rest of the side of the duct we assume that the sheet metal is infinitely smooth and rigid, which is modelled by $Z = \infty$ or $\mathbf{n} \cdot \nabla p = 0$ in (3).

The geometry of the duct makes it logical to use cylindrical coordinates r, θ and z as indicated in Figure 4.

We shall consider only situations where all the data are independent of

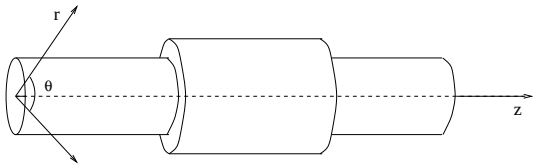

Figure 4: A coordinate system for the duct.

the angular coordinate θ. Therefore we may assume that the pressure p is independent of the angle as well. Rewriting the Laplace operator in cylindrical coordinates, Helmholtz equation thus reduces to

$$\frac{1}{r}(rp_r)_r + p_{zz} + k^2 p = 0 \tag{4}$$

where the sub indices refer to partial derivation with respect to r and z respectively.

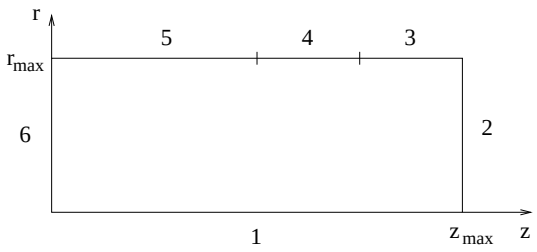

Figure 5: The boundary divided into relevant segments. The z axis is a symmetry axis in the r direction.

The computational domain is reduced to that in Figure 5 and we get the following boundary conditions to (4)

$p_r = 0$	on segment 1 (the centre of the duct)	(symmetry in the r direction)
$p_z = -ikp$	on segment 2 (the outlet)	($Z = \rho c$)
$p_r = 0$	on segment 3 and 5 (stiff walls)	($Z = \infty$)
$p_r = -\frac{i\omega\rho}{Z_s}p$	on segment 4 (the silencer)	(Z_s dependent on the silencer and the frequency)
$p = p_I$	on segment 6 (the source)	(given inlet pressure).

5.3 Variational formulation

Equation (4) is multiplied by r and a test function χ and is then integrated over the r, z domain, corresponding to multiplying Helmholtz equation (2) by χ and integrating over the cylindrical duct volume. This gives

$$\int_0^{z_{max}} \int_0^{r_{max}} (rp_r)_r \chi dr dz + \int_0^{z_{max}} \int_0^{r_{max}} rp_{zz}\chi dr dz + k^2 \int_0^{z_{max}} \int_0^{r_{max}} rp\chi dr dz = 0.$$

Integration by parts taking the boundary conditions of $p_r = 0$ into account and assuming that χ vanishes along the inlet boundary where $z = 0$ gives

$$-\int_0^{z_{max}} \int_0^{r_{max}} rp_r\chi_r dr dz + \int_{z_1}^{z_2} r_{max}p_r(z, r_{max})\chi(z, r_{max})dz - \int_0^{z_{max}} \int_0^{r_{max}} rp_z\chi_z dr dz +$$

$$+ \int_0^{r_{max}} rp_z(z_{max}, r)\chi(z_{max}, r)dr + k^2 \int_0^{z_{max}} \int_0^{r_{max}} rp\chi dr dz = 0 \qquad (5)$$

where z_1 is the inlet coordinate and z_2 is the outlet coordinate of the silencer on the z axis.

In view of the boundary conditions along boundary segments 2 and 4, we may rewrite (5) as

$$-\int_0^{z_{max}}\int_0^{r_{max}} rp_r\chi_r drdz - \int_{z_1}^{z_2} r_{max}\frac{i\omega\rho}{Z_s}p(z,r_{max})\chi(z,r_{max})dz - \int_0^{z_{max}}\int_0^{r_{max}} rp_z\chi_z drdz$$

$$-\int_0^{r_{max}} rikp(z_{max},r)\chi(z_{max},r)dr + k^2\int_0^{z_{max}}\int_0^{r_{max}} rp\chi drdz = 0. \qquad (6)$$

5.4 The Finite Element Method

In the finite element method the pressure p is approximated by a function P which is piecewise linear in r, z on a triangulation of the computational domain as shown in Figure 6. At the nodes along boundary segment 6 we require that P equals p_I which were the given boundary values of p.

To determine the remaining node values of P we use the variational formulation (6), replacing p by P, and choose $\chi = \varphi_j$ for all j such that φ_j vanish along boundary segment 6, which was required of χ in the derivation of (6).

We then get a variational formulation as below.

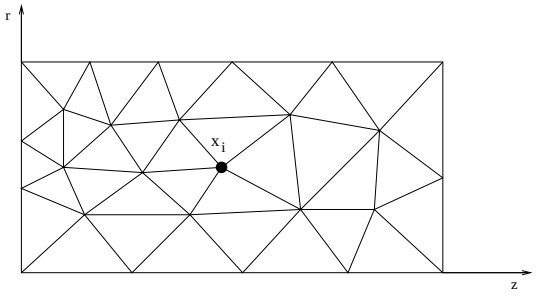

Figure 6: A grid with the node point x_i.

Find the pressure P as above such that for all $\varphi = \varphi_j$

$$\int_0^{z_{max}}\int_0^{r_{max}} rP_r\varphi_r drdz + \int_0^{z_{max}}\int_0^{r_{max}} rP_z\varphi_z drdz - k^2\int_0^{z_{max}}\int_0^{r_{max}} rP\varphi drdz +$$

$$+\frac{i\omega\rho}{Z_s}\int_{z_1}^{z_2} r_{max}P(z,r_{max})\varphi(z,r_{max})dz + ik\int_0^{r_{max}} rP(z_{max},r)\varphi(z_{max},r)dr = 0. \tag{7}$$

If we put $P = \sum_{i=1}^{N} p_i\varphi_i$ we get

$$\sum_{i=1}^{N} p_i \int_0^{z_{max}}\int_0^{r_{max}} r\varphi_{ir}\varphi_{jr}drdz + \sum_{i=1}^{N} p_i \int_0^{z_{max}}\int_0^{r_{max}} r\varphi_{iz}\varphi_{jz}drdz - k^2\sum_{i=1}^{N} p_i \int_0^{z_{max}}\int_0^{r_{max}} r\varphi_i\varphi_j drdz +$$

$$+\frac{i\omega\rho}{Z_s}\sum_{i=1}^{N} p_i \int_{z_1}^{z_2} r_{max}\varphi_i(z,r_{max})\varphi_j(z,r_{max})dz + ik\sum_{i=1}^{N} p_i \int_0^{r_{max}} r\varphi_i(z_{max},r)\varphi_j(z_{max},r)dr = 0.$$

Recalling that the node values $p_i = P(x_i)$ along boundary 6 are given, this is a system of equations $A\mathbf{P} = 0$ with the same number of unknowns as equations. A is the so called stiffness matrix with contribution from the boundary integrals and $\mathbf{P}$ contains the node values p_i.

5.5 Remodelling of the source because of reflections

In the model described above the given data along boundary segment 6 acts as a source creating waves travelling through the duct in the positive z direction. Waves will partly be reflected, for example at the entrance to the silencer, and turn back. Back at the source they will be reflected again and so forth. This is a problem when the computational results are compared to measurements where the measurement setup has been such that waves in the negative direction are absorbed. Therefore we have considered the case when the source is modelled by a source term f in the wave equation and put absorbing boundary conditions at the inlet, similar to those at the outlet, of the form $p + \frac{1}{i\omega\rho}Z\mathbf{n}\cdot\nabla p = 0$ with $Z = \rho c$. The wave equation becomes

$$\Delta\hat{p} - \frac{1}{c^2}\frac{\partial^2\hat{p}}{\partial t^2} = f,$$

where $f = \delta e^{-i\omega t}$ and δ is a function equals ∞ at segment 6 and 0 elsewhere. This gives the Helmholtz equation

$$\Delta p + k^2 p = \delta.$$

The boundary conditions are now

$p_r = 0$	on segment 1
$p_z = -ikp$	on segment 2 and 6
$p_r = 0$	on segment 3 and 5
$p_r = -\frac{i\omega\rho}{Z_s}p$	on segment 4.

The difference in the variational formulation for this model is that equation (7) has two more terms, one from the new source term δ, and one from the new boundary condition at boundary segment 6 and that the test functions φ_j are not required to vanish along segment 6.

6 A Matlab implementation

6.1 Geometry

The computational domain is specified by listing the z and r coordinates for the two end points of each segment of the boundary. These data are stored column wise in a matrix `g`.

6.2 Mesh generation

From the geometry matrix `g` the function `initmesh` in Matlab's PDE tool box generates a triangulation of the domain described in terms of three matrixes `p,t` and `e`. The matrix `p` is a 2×N matrix of all the z and r values for the nodes, `t` is a matrix with one column for each triangle in the mesh specifying its three node numbers which is the column number in `p` for the node's r and z values, and `e` similarly describes the triangle edges coinciding with the boundary of the domain.

The fineness of the mesh may be controlled by the user of the program by giving a parameter to the function `initmesh`.

6.3 Forming and solving discrete system of equations

The integrals in the finite element stiffness matrix A may easily be computed exactly in this case, because the integrand is a polynomial of degree at most three on each element. The matrix is stored as a sparse matrix.

Matlab solves the resulting system of equations $A\mathbf{P} = 0$ using Gaussian elimination.

6.4 Energy evaluation

To evaluate the efficiency of a silencer we study the energy loss in the system. We compare the total wave energy at the outlet cross section of the duct without the silencer to a computation with the silencer installed. The energy is proportional to

$$\int_{\Omega} |P|^2 dxdy = 2\pi \int_0^{r_{max}} r|P|^2 dr,$$

where Ω is the cross section of the duct.

Sound pressure is measured in pascals (Pa), but since the human ear can register pressure in the wide range of 20 μPa to 200 Pa, it is common to use a logarithmic scale and measure the sound pressure by $L_p = 20 \log \frac{|p|}{|p_0|}$, where $p_0 = 20\mu Pa$ is a reference pressure corresponding to $L_p = 0$.

The sound pressure levels are computed for three frequencies for each third octave. They are put together as the following mean value

$$L_{p_{mean}} = 10 \log(10^{L_{p,1}/10} + 10^{L_{p,2}/10} + 10^{L_{p,3}/10}) - 10 \log(3),$$

where $L_{p,i}$ is the sound pressure level for frequency f_i.

6.5 Sound pressure performance

Computations of the sound pressure wave in ducts with and without a silencer are visualized in Figure 7 respective 8. Notice how the silencer reduces the sound pressure wave in Figure 8.

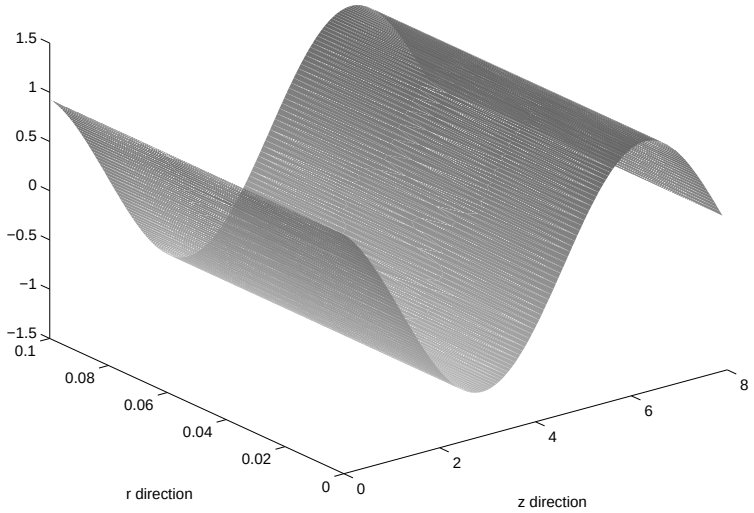

Figure 7: The real part of computed sound pressure in a duct with length 7,9 m and a radius of 0,1 m.

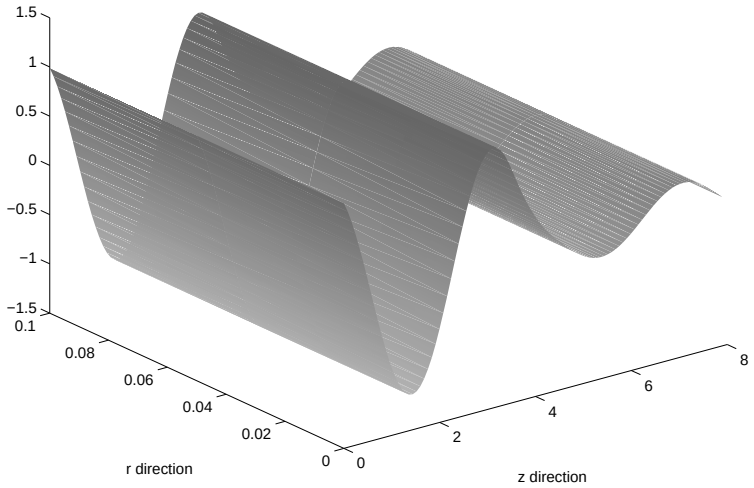

Figure 8: The real part of computed sound pressure in a ducted silencer. The silencer length is 0,9 m, the ducts before and after the silencer are both 3,5 m and the radius is 0,1 m.

7 Impedance modelling

7.1 Silencer

For the computational modelling one needs to find out the acoustic impedance Z of the absorbing material of the silencer, including the perforated sheet metal. For the material, assuming infinite thickness, we may in the literature[3] find the model

$$Z_{inf} = \rho c(1 + 9,08(\frac{1000f}{\sigma})^{-0,75} + i11,9(\frac{1000f}{\sigma})^{-0,73}),$$

where σ is the flow resistivity of the material. For finite thickness t_{abs} we get[4]

$$Z_{abs} = iZ_{inf}\cot(t_{abs}\kappa) \tag{8}$$

where

$$\kappa = \frac{\omega}{c}(1 + 10,8(\frac{1000f}{\sigma})^{-0,7} + i10,3(\frac{1000f}{\sigma})^{-0,59}.$$

From the cavities in the perforated sheet metal we get additional impedance caused by the reactive momentum force of the moving air in the cavities of the form[5]

$$Z_{metal} = -i\omega\rho\frac{A_{ref}}{A_{cav}}(t_{metal} + 0,6r_{cav}), \tag{9}$$

where A_{ref} is an arbitrary reference area of the perforated metal, A_{cav} is the cavity area of A_{ref}, t_{metal} is the thickness of the perforated metal and r_{cav} is the radius of the cavities. There seems to be different opinions of what the coefficient in (9) should be. Another source[6] claims that the coefficient should be 1,7 rather than 0,6.

The impedances Z_{abs} and Z_{metal} may be added together and taken as the impedance of the silencer lining.

Another possibility is to measure the impedance of the absorbing material and perforated sheet metal directly. Such a measurement has been made for this report and is described in section *8.2 Measurements of acoustic impedance* and compared to acoustic impedance data obtained from the model (8) and (9) in Figure 26 in the same section.

[3] Ögren and Jonasson, 1998
[4] Ögren and Jonasson, 1998
[5] Beranek, 1986
[6] Lindblad, 1982

7.2 Reflection at the outlet

For the purpose of comparison with experimental results we have also considered the case of the ventilation duct ending in a big room. To account for the reflections of the waves entering the outlet of a duct ending in an infinite half space (corresponding to a big room) the boundary conditions at the outlet is modified from ρc to[7]

$$Z_{outlet} = \rho c(1 - \frac{J_1(2kr_{max})}{kr_{max}} + i\frac{4}{\pi}\int_0^{\pi/2} \sin(2kr_{max}\cos(\alpha))\sin^2(\alpha)d\alpha),$$

where J_1 is the Bessel function of the first order.

8 Measurement methods

The computational evaluations of the sound pressure reduction of the silencer is validated by comparison to experimental data. There are several measurements made at SP and one is described below. A measurement of the acoustic impedance of the material in the silencer is also made and described below.

8.1 Measurement of sound reduction

According to ISO 7235:1991 sound reduction is measured by comparing the sound pressure at the outlet with and without a silencer installed.

8.1.1 Equipment

The equipment for measuring sound reduction of a silencer consists of a source producing noise, a silencer, two ducts transporting sound waves to and from the silencer, a transmission element (a horn) ending in a reverberation room, six microphones and a computer receiving and processing data. The test setup is shown in Figure 9.

The type of silencer considered here is mainly dissipative, that is, transforms most of the sound energy into heat.

To focus all interest on the quality of the silencer we wish to have as little influence of the rest of the equipment as possible. The horn has the

[7] Beranek, 1986

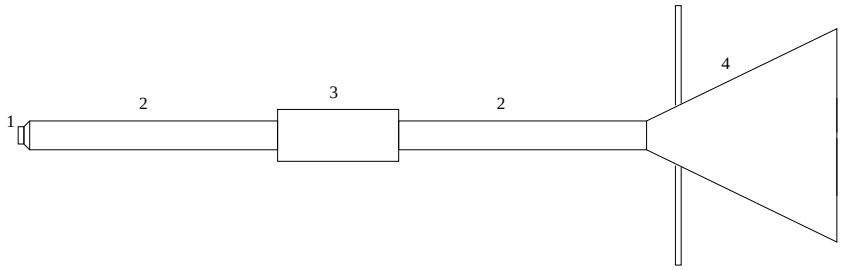

Figure 9: Equipment for measuring sound reduction: (1) source producing noise, (2) duct guiding the sound waves, (3) silencer, (4) transmission element

purpose to remove reflections at the outlet and make the sound pressure waves continue through the horn and into the reverberation room. The horn must, according to ISO 7235:1991, have a total angle not greater than 15° to keep eventual air flow laminar and an outlet area of at least 2 m^2 to make the sound waves adjust to a larger volume with no reflections. In the mathematical formulation this is modelled with the acoustic impedance $Z = \rho c$, as in section *5.2 Boundary conditions*.

In the reverberation room, where the horn terminates, there are six microphones. Each microphone measures the sound pressure over a certain time, normally 30 seconds, and the result is presented as a mean value over time and the six microphones.

The source produces a spectrum of frequencies from 50 Hz to 10 000 Hz.

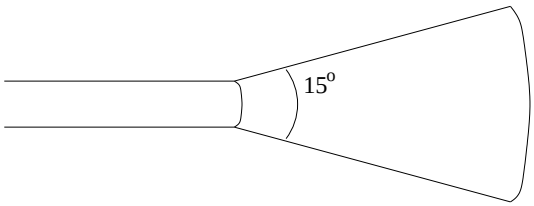

Figure 10: The horn must have a total angle not greater than 15°.

8.1.2 Measurement by ISO 7235:1991

Three different experimental setups are needed to get accepted results according to ISO 7235:1991. One with the silencer installed, one where the

silencer is replaced by a piece of duct and the last one with this piece of duct blocked and filled with absorbing material that will totally stop the sound wave through the duct. The last measurement is important for finding out how much sound is leaking into the reverberation room from the source and the duct through the outside. This kind of transmission is called flanking transmission. If it is unacceptably high the reverberation room must be better isolated.

The difference between the sound pressure level L_p without the silencer and with the silencer installed is called the insertion loss, IL, that is, IL is twenty times the logarithm of the ratio of the sound pressures,

$$IL = Lp_{without} - Lp_{with} = 20 \log \frac{|p_{without}|}{|p_{with}|}.$$

The sound pressure reduction due to the insertion loss is most efficient in the mid frequency band, see the figures in for example chapter *9 Validation of the computational model* . These frequencies include human speech (200-2000 Hz). The problem is to make a silencer that also reduces the sound pressure level at low frequencies. Noise from ventilation system in the lower frequency spectra, mostly about 50 Hz to 250 Hz, are not that efficiently absorbed by the silencer, which is a problem. Higher frequencies are not generated to the same extent as lower frequencies and they are more easily absorbed.

8.2 Measurement of acoustic impedance

The acoustic impedance for different materials can be measured in an apparatus called an impedance tube. The sample used in the reported measurement is the material in the silencer used for the measurement in section *8.1 Measurement of sound reduction.*

8.2.1 Equipment

The method uses a narrow tube, a sample of the sound absorbing material, two microphones put a small distance apart along the tube, a source, and a computer collecting and processing data, see Figure 11.

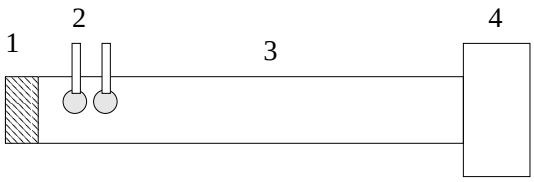

Figure 11: Equipment for measuring impedance in material: (1) sample, (2) microphones, (3) tube and (4) sound source.

8.2.2 Measurement

The microphones are phase calibrated and put into the tube a small distance from each other. The sample which is a piece of the material from the silencer used in the measurement described in section *8.1 Measurement of sound reduction* is put at the end of the tube. The tested material consisted of 95 mm absorbing material, a thin fibrous layer and a perforated sheet metal. Plane waves are sent in from the source.

The waves are reflected and standing waves arise. If no energy is absorbed, which means there is total reflection, the sound pressure is zero in the nodes of the standing waves (the solid curve in Figure 12). When there is some absorption the sound pressure gets a nonzero value in the nodes (the dashed curve in Figure 12).

One measuring method uses a mobile microphone that could be put into the impedance tube. The first maximum and minimum of the sound pressure is found manually and by the value in these points the absorption is calculated.

The two microphone method uses the microphones' ability, after signal processing, to measure sound pressure of waves in both directions to get the absorption of the sample.

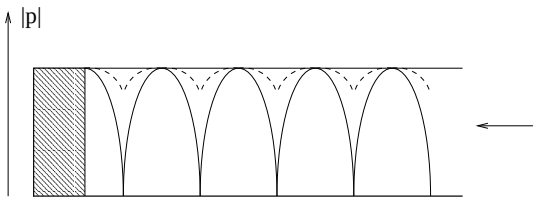

Figure 12: The absolute sound pressure $|p|$ in an impedance tube for absorption (dashed line) and total reflection (the solid line) at the sample.

9 Validation of the computational model

There are three types of experimental setups used at SP. The differences between them are the source setup and the transmission element. Figure 13 shows the setup according to ISO 11691:1995. It has a reflecting source and ends in a half space. In Figure 14 a setup according to ISO 7235:1991 is shown. The source is reflecting, but the ducted silencer now ends in a transmission element. This setup was used in the measurement described in section *8.1.2 Measurement by ISO 7235:1991*. The source in the setup shown in Figure 15 is absorbing and the ducted silencer ends in a half space. The method based on this experimental setup is called the GLSM method and was used in Sweden before ISO 11691:1995 was introduced.

To make a validation of the computational model we compare measurement results from the three experimental setups and one of the acoustic impedance with computational results with the same parameters.

The plots are mostly presented in one third octaves here, but some are even presented in octaves. The parameters are listed in section *14.1 Parameters for validation of the model* in Appendix.

The flow resistivity is a sensitive parameter. It can even vary between silencers with the same design. The value depends among other things on how hard the material is compressed. This value is written in the figure text for each figure.

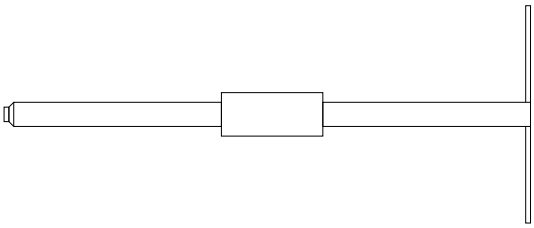

Figure 13: Experimental setup according to ISO 11691:1995.

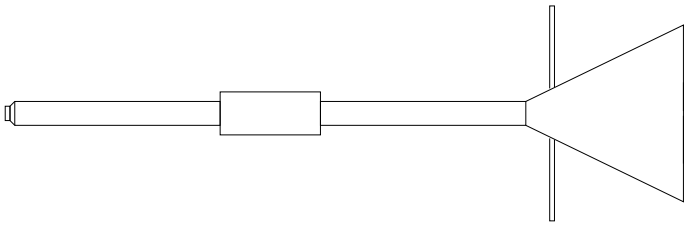

Figure 14: Experimental setup according to ISO 7235:1991.

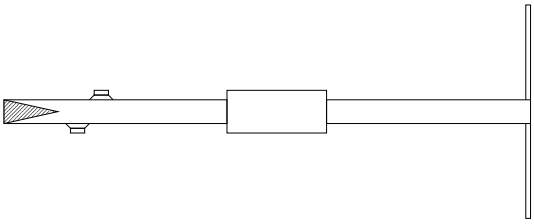

Figure 15: Experimental setup according to the GLSM method.

9.1 Comparison for setup according to ISO 11691:1995

Figure 16 and 17 indicates that we have bad coincidence of the measured and computed result for the setup according to ISO 11691:1995 at the lower frequencies but good at the middle frequencies.

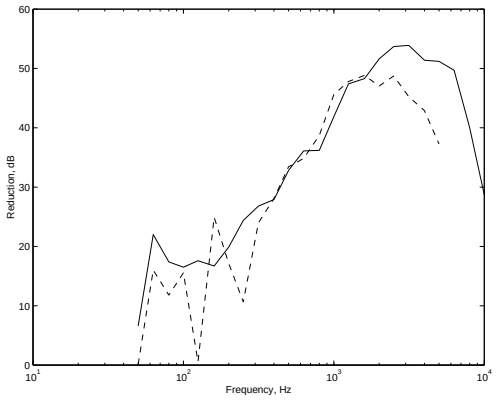

Figure 16: Measured (-) and computed (- -) sound pressure level reduction for the setup according to ISO 11691:1995, with the silencer length 0,7 m and the radius 0,0625 m. The flow resistivity is 37000 Nsm^{-5} and the cut-on frequency is 1578 Hz.

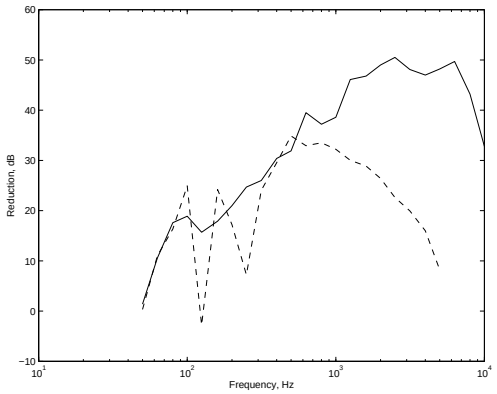

Figure 17: Measured (-) and computed (- -) sound pressure level reduction for the setup according to ISO 11691:1995, with the silencer length 0,7 m and the radius 0,0625 m. The flow resistivity is 20000 Nsm^{-5} and the cut-on frequency is 1578 Hz.

9.2 Comparison for setup according to ISO 7235:1991

Comparison between the measured and computed result for the setup according to ISO 7235:1991 indicates quit good coincidence in the frequency spectra under the cut-on frequency, see Figure 18, 19 and 20.

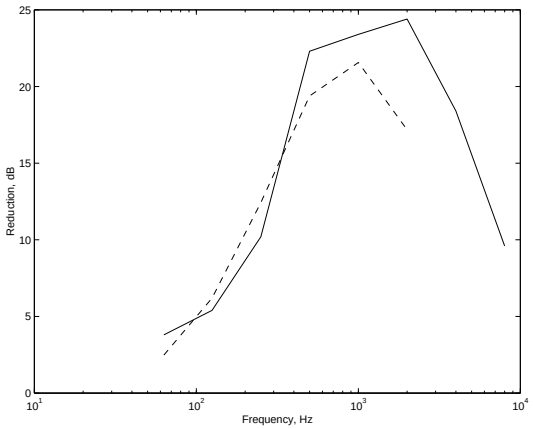

Figure 18: Measured (-) and computed (- -) sound pressure level reduction for the setup according to ISO 7235:1991, with the silencer length 1,2 m and the radius 0,125 m. No perforated sheet metal is used. The flow resistivity is 60000 Nsm^{-5} and the cut-on frequency is 789 Hz.

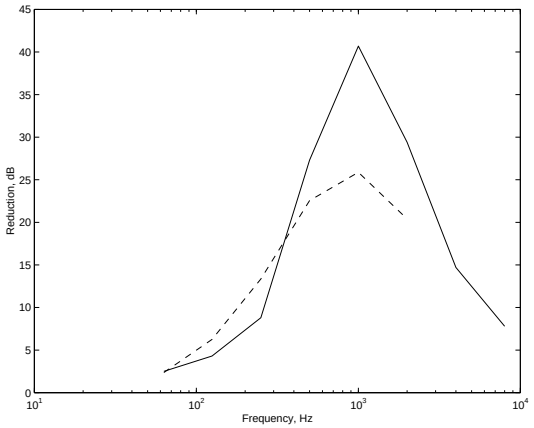

Figure 19: Measured (-) and computed (- -) sound pressure level reduction for the setup according to ISO 7235:1991, with the silencer length 1,2 m and the radius 0,125 m. The flow resistivity is 50000 Nsm^{-5} and the cut-on frequency is 789 Hz.

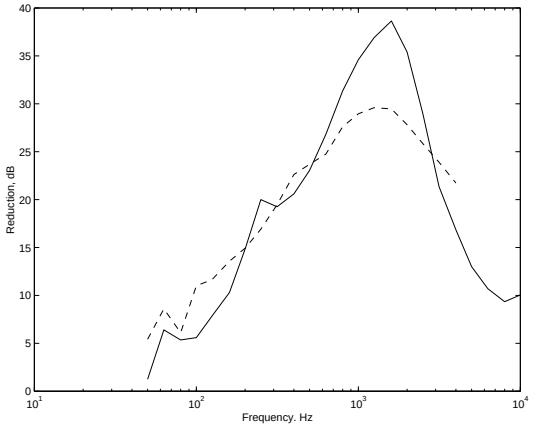

Figure 20: Measured (measurement described in section *8.1 Measurement of sound reduction*) (-) and computed (- -) sound pressure level reduction with the silencer length 0,9 m and the radius 0,1 m. The flow resistivity is 50000 Nsm^{-5} and the cut-on frequency is 986 Hz.

9.3 Comparison for setup according to the GLSM method

Comparison for the setup according to the GLSM method gives good coincidence of the result from the computed and measured case for frequencies up to about the cut-on frequency, see Figure 21, 23 and 24. Figure 22 has coincidence for spectra up to about 2000 Hz.

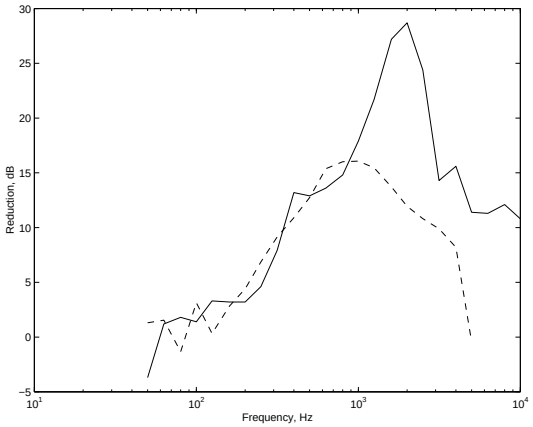

Figure 21: Measured (-) and computed (- -) sound pressure level reduction for the setup according to the GLSM method, with the silencer length 0,6 m and radius 0,125 m. The flow resistivity is 40000 Nsm^{-5} and the cut-on frequency is 789 Hz.

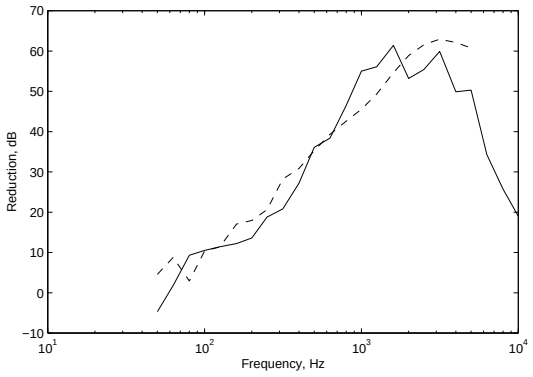

Figure 22: Measured (-) and computed (- -) sound pressure level reduction for the setup according to the GLSM method, with the silencer length 0,9 m and radius 0,05 m. The flow resistivity is 80000 Nsm^{-5} and the cut-on frequency is 1972 Hz.

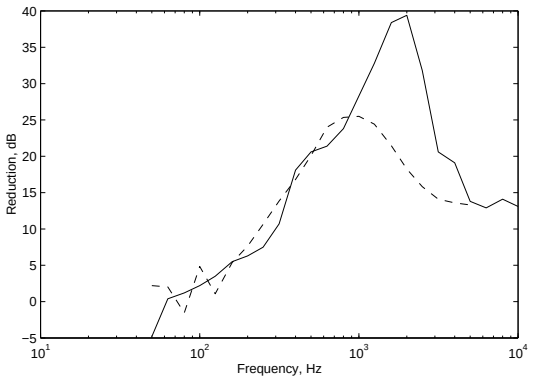

Figure 23: Measured (-) and computed (- -) sound pressure level reduction for the setup according to the GLSM method, with the silencer length 0,9 m and radius 0,125 m. The flow resistivity is 37000 Nsm^{-5} and the cut-on frequency is 789 Hz.

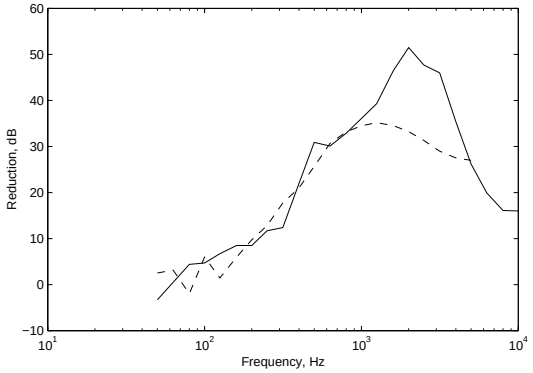

Figure 24: Measured (-) and computed (- -) sound pressure level reduction for the setup according to the GLSM method, with the silencer length 0,9 m and radius 0,08 m. The flow resistivity is 60000 Nsm^{-5} and the cut-on frequency is 1233 Hz.

9.4 Validation of the silencer impedance model

An absorption coefficient (Figure 25) and a reflection constant is given for each frequency band in the range 50 to 1600 Hz as a result of the measurement of the acoustic impedance described in *8.2 Measurement of acoustic impedance*. The result and a comparison with an acoustic impedance model (see Equation (8) in section *7.1 Silencer*) is shown in Figure 26. The acoustic impedance is listed in section *14.1 Parameters for validation of the model* in Appendix.

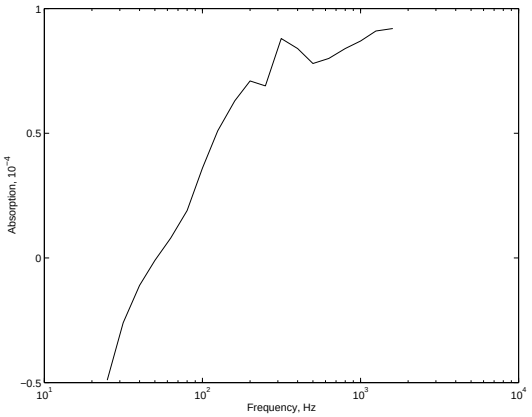

Figure 25: Absorption curve for the sample in the measurement of the acoustic impedance.

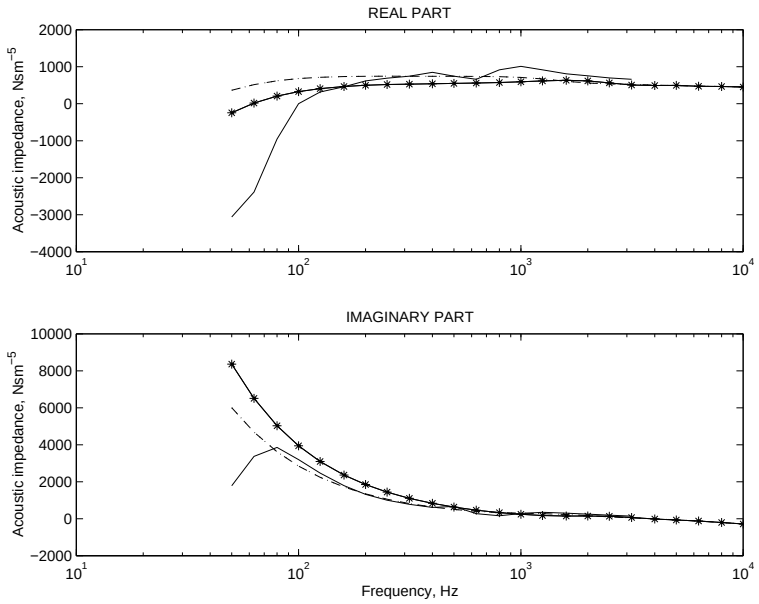

Figure 26: The real and imaginary part for the measured (-) and calculated acoustic impedance with the flow resistivity of 30000 Nsm^{-5} and a thickness of the absorbing material of (*) 5 cm and (- -) 7 cm.

9.5 Cut-on frequency

We have plane waves for frequencies up to a point where the wave length is equal to 0,58 times the duct diameter[8] ($\lambda = 0,58d$). This frequency is called the cut-on frequency and is derived from theoretical studies of the wave equation. Over the cut-on frequency non-axial wave modes can propagate. We model only plane waves at the source and since non-axial modes are reduced much better in the silencer than plane waves the experimental results get better reduction over the cut-on frequency than the computational result.

9.6 Low frequency performance

There is oscillation of the curves at the lower frequencies in almost every calculation done. That is caused by standing waves that are created by reflections of waves at for example the inlet of the silencer. These waves are created by change in boundary conditions. The effect is not that obvious in the measurements because this is smoothened out in the non ideal case.

[8]ISO 10534, 1996

By remodelling the source in section *5.5 Remodelling of the source because of reflections* these oscillations are becoming less significant, but are still visible (Figure 27).

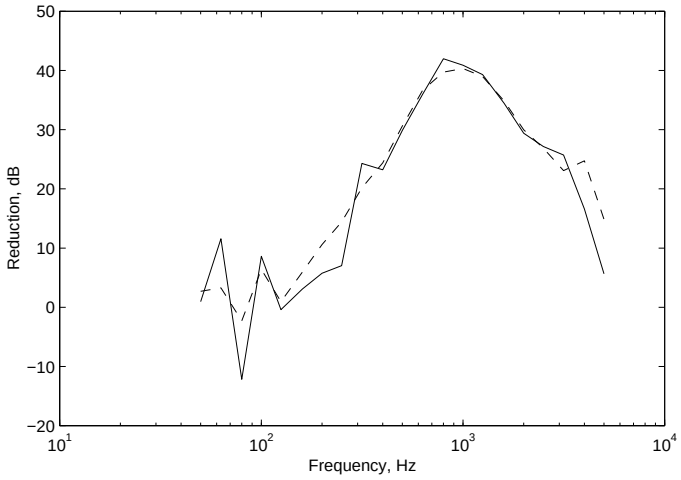

Figure 27: The sound pressure reduction with reflection (-) and without reflection at the source (- -). The silencer length is 0,9 m and the radius is 0,1 m. The cut-on frequency is 986 Hz.

10 Parametric study

With a computational tool available we can now study the propagation of sound through a silencer, evaluate the performance of a given silencer design, and vary parameters in a search for an as optimal design as possible.

The study concerns the setup according to the GLSM method with an absorbing source and the duct ending in a half space.The parameters of the following figures are listed in section *14.2 Parameters for parameter study* in Appendix.

10.1 Length of the silencer

As we can see in Figure 28 the length of the silencer has a big impact on the result. A length doubling gives over 10 dB difference in the reduction for frequencies over approximately 200 Hz.

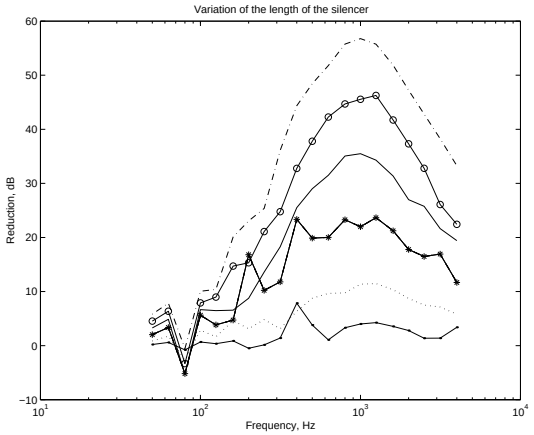

Figure 28: The length of the silencer is varied between (.) 0,1 m; (...) 0,3 m; (*) 0,6 m; (-) 0.9 m; (o) 1,2 m and (-.-) 1,5 m and the radius is 0,1 m. The cut-on frequency is 986 Hz.

10.2 Length of the ducts

Change in the length of the duct between the source and the silencer makes little difference in the reduction, see Figure 29. The reduction is strengthened or weakened because of standing waves in the duct. When the length of the duct between the silencer and the outlet is varied, these phenomena are moved from one frequency to another (Figure 30). If the experimental setup had the transmission element change in this piece of duct would not have impact.

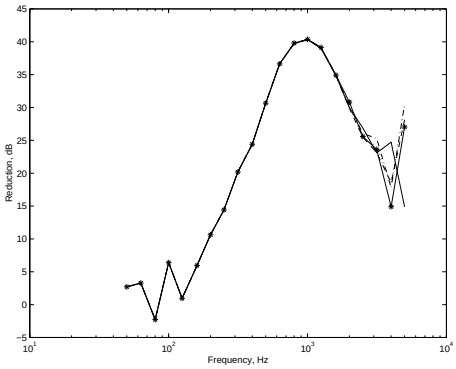

Figure 29: The length of the duct between the source and the silencer is varied between (- -) 2,0 m; (...) 2,5 m; (.-.-) 3,0 m, (-) 3,5 m and (*) 4,0 m, the silencer length is 0,9 m and the radius is 0,1 m. The cut-on frequency is 986 Hz.

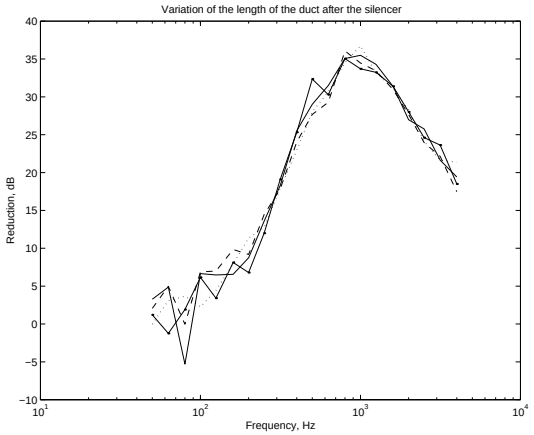

Figure 30: The length of the duct between the silencer and the outlet is varied between (.) 2,0 m; (...) 2,5 m; (- -) 3,0 m and (-) 3,5 m, the silencer length is 0,9 m and the radius is 0,1 m. The cut-on frequency is 986 Hz.

10.3 Radius of the ducts

The radius of the duct has an impact on the sound pressure reduction, the smaller radius the better reduction (Figure 31).

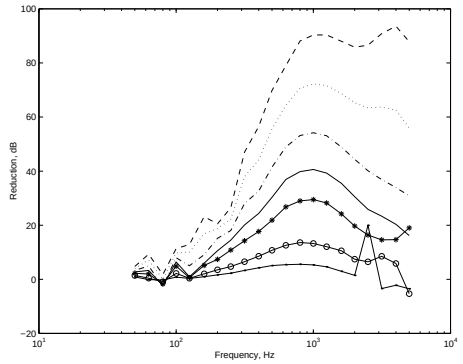

Figure 31: The radius of the duct is varied between (- -) 0,05 m; (...) 0,0625 m; (-.-) 0,08 m; (-) 0,10 m; (*) 0,125 m; (o) 0,20 m and (.) 0,315 m and the silencer length is 0,9 m. The cut-on frequency is respectively 657 Hz, 986 Hz, 1409 Hz and 1972 Hz.

10.4 The perforated sheet metal

When the hole radius of the perforated sheet metal is varied we see little change in reduction at the lower frequencies (Figure 32).

The same is true when the amount of hole, represented as the hole percent, is varied (Figure 33) and similarly when the thickness of the perforated sheet metal is varied (Figure 34).

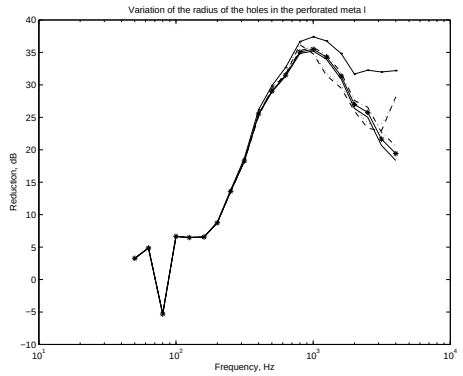

Figure 32: The hole radius is varied with (- -) 0,5 mm; (...) 1,0 mm; (*) 2,0 mm; (.) 5,0 mm and (-) 1,5 mm, the silencer length is 0,9 m and the radius is 0,1 m. The cut-on frequency is 986 Hz.

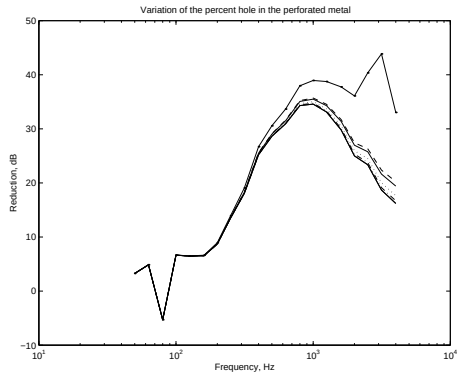

Figure 33: Variation of the hole percentage of the perforated sheet metal (-) 90 %; (-.-) 70 %; (...) 50 %; (-) 34 %; (- -) 30 % and (.) 10 %, the silencer length is 0,9 m and the radius is 0,1 m. The cut-on frequency is 986 Hz.

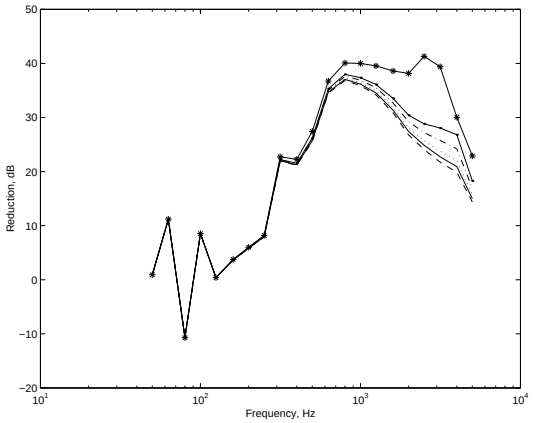

Figure 34: The thickness of the perforated metal is varied with (- -) 0,4 mm; (-) 0,7 mm; (...) 1,0 mm; (-.-) 1,5 mm; (.) 2,0 mm and (*) 5,0 mm, the silencer length is 0,9 m and the radius is 0,1 m. The cut-on frequency is 986 Hz.

10.5 Flow resistivity and the thickness of the absorbing material

The flow resistivity and the thickness of the absorbing material are sensitive parameters (Figure 35). There is a certain value of flow resistivity for each thickness of the absorbing material that gives maximum reduction of the sound pressure level. Higher and lower values than that gives less reduction.

When the thickness is as long as a certain wavelength standing waves arise in the absorbing material, which has a big effect on the result (Figure 36).

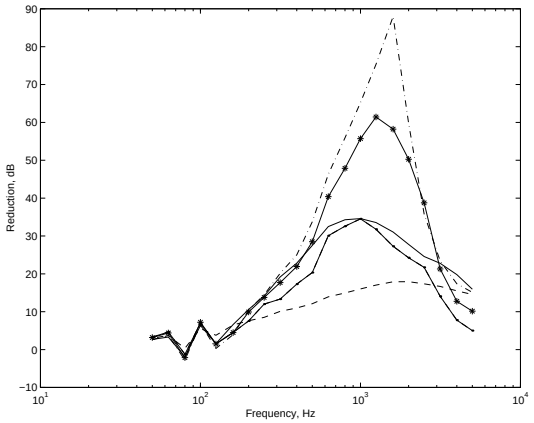

Figure 35: Variation of the flow resistivity with the values (.) 1000, (*) 3700, (-.-) 10000;, (-) 37000 and (- -) 100000 Nsm^{-5} for 5 cm absorbing material. The silencer length is 0,9 m and the radius is 0,1 m. The cut-on frequency is 986 Hz.

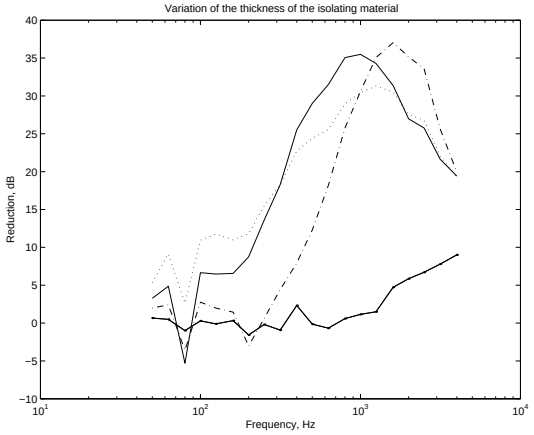

Figure 36: The thickness of the absorbing material is varied between (.) 10 cm; (-.-) 30 cm; (-) 50 cm and (...) 100 cm for flow resistivity 37000 Nsm^{-5}. The silencer length is 0,9 m and the radius is 0,1 m. The cut-on frequency is 986 Hz.

11 Conclusion

Modelling the sound propagation in a duct by the finite element method gives a computational tool to for example study the performance of a given silencer design. That gives the possibility to compare experimental results for the insertion loss with computational results. This showed good coincidence at the frequencies below the cut-on frequency.

We may also study the impact of different parameters on the sound pressure reduction. It was seen that the duct length, the duct radius and the flow resistance together with the thickness of the material in the silencer are parameters that with small changes has big impact on the reduction of sound pressure.

There is also a possibility to generally study the evolution of sound pressure through a silencer.

12 Discussion

Because of the small width compared to the length of the duct/silencer domain the meshing tends to create few elements in the r direction. This combined with the homogeneous Neumann conditions at $r = 0$ and $r = r_{max}$, gives few degrees of freedom in the r direction, unless the mesh is fine enough.

High frequencies have small wave length which requires a fine mesh, and consequently more computational resources.

To reduce execution time one could of course use parallel computing since the reduction of sound pressure is computed separately for each frequency.

A posteriori error analysis are available for the finite element method for Helmholtz equation[9]. It would therefore be possible to get a bound for the computational error on a given level through adaptive refinements of the mesh.

There are other numerical methods that could be used to solve Helmholtz equation. For example one could use quadratic elements instead of triangular or raise the order of approximations by using higher degree piecewise polynomials. One could also use a boundary element method based on a

[9]Larsson, 1999

reformulation of the given boundary value problem as an integral equation.

To further improve the model in this report one could remodel the source to create waves with non-axial modes to get better agreement with experimental results at higher frequencies.

It would be interesting to continue the parameter study trying to find the design of the "perfect silencer".

13 References

Beranek, Leo L., 1986 (third printing 1988), *Acoustics*, Acoustic Society of America, New York

Cuvelier, C., Segal, A. and van Steenhoven, A. A., 1986, *Finite Element Methods and Navier-Stokes Equations*, D. Reidel Publishing Company, Dordecht, Holland

Delany, M. E. and Bazley, E. N., 1969, *Acoustical Properties of Fibrous Absorbent Materials*, National Physical Laboratory, Teddington, Middlesex

Ingård, Uno, 1974, *Fysikaliska principer vid bullerreduktion: Egenskaper hos ljudkällor och deras ljudfält*, Lunds tekniska högskola, Lund

Jonasson, Hans, 1998, *Ingenjörsakustik*, SP, Borås

Kinsler, Lawrence E., Frey, Austin R., Coppens, Alan B., Sanders, James V., 1982, *Fundamentals of Acoustics*, John Wiley & Sons, Canada

Larsson, Mats G., 1999, *A new error analysis for finite element approximations of indefinite linear elliptic problems*, Department of Mathematics, Chalmers University of Technology, Göteborg

Lindblad, Sven G., 1982, *Akustik IV*, Lunds tekniska högskola, Lund

Morse, Philip M., 1976 (third printing 1986), *Vibration and sound*

Ögren, Mikael and Jonasson, Hans, 1998, *Measurement of the Acoustic Impedance of Ground*, SP Swedish National Testing and Research Institute, Borås

Ögren, Mikael, 1998, *Ljudutbredning ovanför Impedans-plan med diskontinuerlig impedansfördelning*, SP, Borås

ISO 7235, 1991, *Acoustics - Measurement procedures for ducted silencers - Insertion loss, flow noise and total pressure loss*

ISO 10534, 1996, *Acoustics - Determination of sound absorption coefficient and impedance in impedance tubes*

ISO 11691, 1995, *Acoustics - Measurement of insertion loss of ducted silencers without flow - Laboratory survey method*

14 Appendix

The parameters for the chapter *9 Validation of the computational model* and the section *10 Parametric study* are listed below.

14.1 Parameters for validation of the model

Parameters for the Figures 16-24, and 26-27 in chapter *9 Validation of the computational model.*

Table to Figure 16

Parameter	**Value**
Silencer length	0,7 m
Duct radius	0,0625 m
Flow resistivity	37000 Nsm^{-5}
Isolating thickness	10 cm
Percent hole in perf. metal	34
Metal thickness	0,7 mm
Hole radius	1,5 mm
Cut-on frequency	1578 Hz

Table to Figure 17

Parameter	**Value**
Silencer length	0,7 m
Duct radius	0,0625 m
Flow resistivity	20000 Nsm^{-5}
Isolating thickness	8 cm
Percent hole in perf. metal	34
Metal thickness	0,7 mm
Hole radius	1,5 mm
Cut-on frequency	1578 Hz

Table to Figure 18

Parameter	**Value**
Silencer length	1,2 m
Duct radius	0,125 m
Flow resistivity	60000 Nsm^{-5}
Isolating thickness	5 cm
Perf. sheet metal	non
Cut-on frequency	789 Hz

Table to Figure 19

Parameter	**Value**
Silencer length	1,2 m
Duct radius	0,125 m
Duct length 1	4,0 m
Duct length 2	3,5 m
Flow resistivity	50000 Nsm^{-5}
Isolating thickness	5 cm
Percent hole in perf. metal	34
Metal thickness	0,7 mm
Hole radius	1,5 mm
Cut-on frequency	789 Hz

The temperature during the measurement described in section *8.1.2 Measurement by ISO 7235:1991* was 19°C and the humidity was 21%. The parameters were:

Table to Figure 20

Parameter	**Value**
Silencer length	0,9 m
Duct radius	0,1 m
Flow resistivity	50000 Nsm^{-5}
Isolating thickness	5 cm
Percent hole in perf. metal	34
Metal thickness	0,7 mm
Hole radius	1,5 mm
Cut-on frequency	986 Hz.

Table to Figure 21

Parameter	**Value**
Silencer length	0,6 m
Duct radius	0,125 m
Flow resistivity	40000 Nsm^{-5}
Isolating thickness	5 cm
Percent hole in perf. metal	34
Metal thickness	0,7 mm
Hole radius	1,5 mm
Cut-on frequency	789 Hz

Table to Figure 22

Parameter	**Value**
Silencer length	0,9 m
Duct radius	0,05 m
Flow resistivity	80000 Nsm^{-5}
Isolating thickness	5 cm
Percent hole in perf. metal	34
Metal thickness	0,7 mm
Hole radius	1,5 mm
Cut-on frequency	1972 Hz

Table to Figure 23

Parameter	**Value**
Silencer length	0,9 m
Duct radius	0,125 m
Flow resistivity	37000 Nsm^{-5}
Isolating thickness	5 cm
Percent hole in perf. metal	34
Metal thickness	0,7 mm
Hole radius	1,5 mm
Cut-on frequency	789 Hz

Table to Figure 24

Parameter	**Value**
Silencer length	0,9 m
Duct radius	0,08 m
Flow resistivity	60000 Nsm^{-5}
Isolating thickness	4 cm
Percent hole in perf. metal	34
Metal thickness	0,7 mm
Hole radius	1,5 mm
Cut-on frequency	1233 Hz

Table to Figure 26

Parameter	**Value**
Flow resistivity	30000 Nsm^{-5}
Isolating thickness	5 and 7 cm
Percent hole in perf. metal	34
Metal thickness	0,7 mm
Hole radius	1,5 mm

The result of the measurement described in section *8.2 Measurement of acoustic impedance* is listed below. The impedance tube had an inner diameter of 100 mm and a length of 1005 mm. The microphones where put 49,8 mm from each other.

Table to Figure 26

Frequency	**Acoustic impedance** ($\mathrm{Nsm^{-5}}$)
25	-3,0603 + 1,7864i
31,5	-2,3880 + 3,3762i
40	-0,9535 + 3,8580i
50	0,0000 + 3,1982i
63	0,3190 + 2,4720i
80	0,4599 + 1,7880i
100	0,6167 + 1,3212i
125	0,6894 + 1,0009i
160	0,7455 + 0,7792i
200	0,8504 + 0,6128i
250	0,7444 + 0,6647i
315	0,6620 + 0,2769i
400	0,9175 + 0,1600i
500	1,0091 + 0,2841i
630	0,9177 + 0,3471i
800	0,8078 + 0,3021i
1000	0,7559 + 0,2503i
1250	0,6977 + 0,1927i
1600	0,6616 + 0,1434i

Table to Figure 27

Parameter	**Value**
Silencer length	0,9 m
Duct radius	0,1 m
Flow resistivity	37000 $\mathrm{Nsm^{-5}}$
Isolating thickness	5 cm
Percent hole in perf. metal	34
Metal thickness	0,7 mm
Hole radius	1,5 mm
Cut-on frequency	986 Hz

14.2 Parameters for the parameter study

The computations in section *10 Parametric study* are made for a duct ending in a half space and with a reflecting source (the setup according to the GLSM method). The parameters in Figures 28-36 have the parameter values in the table below unless the parameter is studied and therefore varied. Those parameter values are described in the figure text.

Table to Figures 28-36

Parameter	**Value**
Silencer length	0,9 m
Duct radius	0,10 m
Flow resistivity	37000 Nsm^{-5}
Isolating thickness	5 cm
Percent hole in perf. metal	34
Metal thickness	0,7 mm
Hole radius	1,5 mm
Cut-on frequency	986 Hz